Fracture strength of implant-supported veneered zirconia crowns with mechanical retentive devices attached to frameworks

Tatsuro Kobayashi

Nihon University Graduate School of Dentistry

(Directors: Prof. Futoshi Komine, Asst. Prof. Junichi Honda)

Contents

This thesis is based on the published article listed below with additional data.

Kobayashi T, Honda J, Kubochi K, Iwasaki T, Watanabe Y, Komine F (2023) Influence of attaching mechanical retentive devices onto frameworks on fracture resistance of implant-supported zirconia crowns. Dent Mater J (in press)

Summary

Metal-ceramic restorations and all-ceramic restorations made of zirconia or lithium disilicate ceramics have been used for implant-supported crowns (ISCs). Implant-supported zirconia crowns (IZCs) exhibited stable survival rates in clinical trials and are currently considered a valid treatment alternative.

Indirect composite resins have been widely used as a layering material for tooth-supported crowns and ISCs. It has been reported that composite resin materials are beneficial in reducing the occlusal stresses compared to layering porcelain for ISCs. Previous study demonstrated that the fracture strength of IZCs, in which an indirect composite resin is veneered onto a zirconia framework, did not differ significantly from metal-ceramic and zirconia restorations.

To increase the mechanical retention of layering composite resins, mechanical retentive devices such as retention beads are attached to a metal framework for resin-veneered restorations. A laboratory study demonstrated that the attachment of mechanical retentive devices to zirconia frameworks yielded adequate bond strength between a layering composite resin and zirconia frameworks. However, only a few studies evaluated the fracture resistance of IZCs with layering composite resins onto facing surfaces attached to mechanical retentive devices.

This study aimed to investigate the fracture resistance of IZCs, in which two layering materials (feldspathic porcelain and indirect composite resin) were layered onto zirconia frameworks with mechanical retentive devices. The null hypothesis to be tested was that attaching mechanical retentive devices onto zirconia frameworks would not affect the fracture load of IZCs.

An implant analogue was used to simulate implant therapy for a missing molar. These implant analogues were axially embedded in acrylic resin using plastic specimen holders.

Titanium implant abutments were tightened to each implant analogue with a torque of 32 N·cm. The abutment-implant complexes were divided into two groups based on the presence or absence of attached mechanical retentive devices on zirconia frameworks (n=44 and 22, respectively).

These complexes were scanned using a laboratory scanner, and the frameworks were designed with 0.5 mm thickness using software. Based on the designed standard triangulated language (STL) data, the frameworks were machine-milled from a pre-sintered zirconia disk using a milling device and subsequently sintered in a furnace at 1,375°C for 90 min.

The surface of the zirconia frameworks was airborne-particle abraded with 50 μm Al_2O_3 particles at a pressure of 0.2 MPa for 10 s, with 10 mm distance between the nozzle and framework surface. The mechanical retentive devices were adjusted to a particle size of 160-180 μm using a sieve. The protocol for attaching different materials of mechanical retentive devices was divided into two groups. The glaze material or the opaque porcelain material was thinly applied onto the surface of the zirconia framework, referred to as the GL group and the OP group, respectively. The group with no attached mechanical retentive devices (ND group) underwent only airborne-particle abrasion.

Feldspathic porcelain and indirect composite resin were employed as layering materials. The feldspathic porcelain was manually layered onto the frameworks and subsequently fired using a SingleMat porcelain furnace following the instructions provided by the manufacturer (FP veneer). For the IC veneer, the frameworks were layered with Estenia C&B, cured using a photopolymerizer, and heat-activated polymerized in an oven. Restorations were fabricated to achieve a standardized configuration with a width of 10.5 mm and a height of 8 mm using a standardized silicone index.

The crowns were then adhesively placed to the implant abutments using a dual-polymerized resin luting material. All specimens were restored in distilled water at 37°C for

24 h before undergoing fracture resistance testing.

A piece of tin foil was inserted between a stainless-steel ball (diameter, 6.0 mm) and the occlusal surface of the specimens. To determine fracture load, all specimens were subjected to perpendicularly loading using a mechanical testing machine at a cross-head speed of 0.5 mm/min until fracture occurred. The break detector threshold was established at a 10% decrease of maximum force.

The distribution and equality of variances were analyzed with the Shapiro-Wilk and Levene tests, using IBM SPSS Statistics. The Shapiro-Wilk test indicated a normal distribution of the data ($p>0.05$), and the Levene test showed the homogeneity of variances ($p>0.05$). To compare the fracture load, Tukey's honestly significant difference test was employed within the same layering material group. A significance level of 0.05 was chosen for all data analyses.

To examine the failure pattern, the fractured surfaces were observed under a stereomicroscope. There were three types of fracture patterns, namely, veneer fracture, interface fracture, and framework fracture. Furthermore, the fractured surfaces were then examined using a scanning electron microscope.

In the FP veneer, the GL group recorded the highest mean fracture load values of 3.00±0.28 kN. The mean fracture load values of the ND group (2.48±0.41 kN) were significantly higher than those of the OP group (1.91±0.48 kN). In the IC veneer, Tukey's honestly significant difference test revealed that the GL (2.62±0.22 kN) and OP (2.88±0.36 kN) groups had significantly higher mean fracture loads than the ND (2.19±0.34 kN) group.

The assessment of the failure pattern of the tested specimens indicated that the framework fracture was frequently observed in the GL and ND groups, irrespective of the veneer used. For the OP groups, a similar occurrence of interface fractures and framework fractures was observed for FP and IC veneers.

For the FP veneer-GL group, the cracked surface of the mechanical retentive devices surrounded by glaze material can be seen. The fracture surface of the FP veneer-OP group exhibited the mechanical retentive devices debonded from the opaque porcelain material. The FP veneer-ND group showed that mixed cohesive fractures of the frameworks and veneers are presented. Similar fracture surface images to those in the FP groups were observed in the IC groups.

In the FP veneer-GL group, SEM images showed that the materials penetrated the undercut of the mechanical retentive devices at the interface between the zirconia framework and the layering material. Conversely, the SEM image of the FP veneer-OP group indicated the absence opaque porcelain material around the mechanical retentive devices.

For the IC veneers, the IC veneer-GL and OP groups showed that the mechanical retentive devices were embedded in the glaze and opaque porcelain materials, respectively.

The FP veneer-GL group showed the fractured surface of the mechanical retentive devices and the mechanical retentive devices in the glaze porcelain material. In contrast, the FP veneer-OP group exhibited the interface fracture between the opaque porcelain materials and the zircon beads. The IC veneer-GL and OP groups indicated fracture within the glaze and opaque porcelain materials.

Within the limitations of this in vitro study, the following conclusions were drawn:

1. The fracture resistance of the IZCs can be improved by applying glaze material before attaching mechanical retentive devices for porcelain layering.
2. For the IC veneer, the GL and OP groups showed significantly higher fracture load values than the ND group.
3. The mechanical interlocking between the zirconia frameworks and the layering materials tested was achieved with the use of mechanical retentive devices.

4. All types of the IZCs tested in this study have the potential to withstand clinical occlusal forces in posterior applications.

Introduction

Implant-supported crowns (ISCs) have frequently been used to replace a single missing tooth. The ISCs have functional, biological, and mechanical advantages, and they exhibit superior clinical survival rates in long-term observations[1)]. Implant therapy for single-tooth replacement is currently one of the most reliable treatment modalities.

Metal-ceramic restorations and all-ceramic restorations made of zirconia or lithium disilicate ceramics have been used for ISCs[1)]. Implant-supported zirconia crowns (IZCs) exhibited stable survival rates in clinical trials and are currently considered a valid treatment alternative. On the contrary, the chipping of the layering porcelain is a common complication of IZCs[2)]. To overcome this issue, several techniques have been validated, including pressed-on-zirconia ceramic restorations[3)], the use of layering indirect composite materials as an alternative to porcelain[4)], and monolithic zirconia restorations[5,6)]. In addition, to achieve long-term clinical success with ceramic restorations, the bond strength between zirconia frameworks and layering materials should be strong and durable. Several methods have been investigated to improve this bond. Airborne-particle abrasion with alumina particles on zirconia frameworks enhances the bond strength with layering porcelain[7,8)]. The use of porcelain liner materials improves the bond between layering porcelains or indirect composite resins and zirconia frameworks[9-12)]. Laser technology represents an alternative approach to surface treatment of zirconia frameworks prior to the application of layering materials. Many studies have shown that surface treatments using lasers, including carbon dioxide[13,14)], neodymium-doped yttrium aluminum garnet[15)], and erbium-doped yttrium aluminum garnet[16,17)], can yield stable bond strength between layering materials and zirconia frameworks. Monolithic zirconia restorations offer several advantages such as a low risk of chipping, a less invasive approach, and low cost, which has resulted in the widespread use of IZCs[6)]. However, there are only a few studies on the medium- and long-term clinical results of implant-supported monolithic zirconia crowns.

Indirect composite resins have been widely used as a layering material for tooth-supported crowns and ISCs. It has been reported that composite resin materials are beneficial in reducing the occlusal stresses compared to layering porcelain for ISCs[18)]. Taguchi *et al*.[4)] demonstrated that the fracture strength of IZCs, in which an indirect composite resin is veneered onto a zirconia framework, did not differ significantly from metal-ceramic and zirconia restorations. Conversely, it is known that composite resins have drawbacks such as inferior wear resistance and poor mechanical properties[19,20)].

To increase the mechanical retention of layering composite resins, mechanical retentive devices such as retention beads are attached to a metal framework for resin-veneered restorations[21,22)]. A laboratory study demonstrated that the attachment of mechanical retentive devices to zirconia frameworks yielded adequate bond strength between a layering composite resin and zirconia frameworks[23,24)]. However, only a few studies evaluated the fracture resistance of IZCs with layering composite resins onto facing surfaces attached to mechanical retentive devices.

This study aimed to investigate the fracture resistance of IZCs, in which two layering materials (feldspathic porcelain and indirect composite resin) were layered onto zirconia frameworks with mechanical retentive devices. The null hypothesis to be tested was that attaching mechanical retentive devices onto zirconia frameworks would not affect the fracture load of IZCs.

Materials and Methods

The materials used and their components in the current study are detailed in Table 1. An implant analogue (diameter, 5.0 mm; Implant replica Brånemark System WP, Novel Biocare, Goteborg, Sweden) was used to simulate implant therapy for a missing molar. These implant analogues were axially embedded in acrylic resin (Technovit 4000, Heraeus Kulzer, Wehrheim, Germany) using plastic specimen holders. Titanium implant abutments (Snappy abutment 5.5 Brånemark System WP; Novel Biocare) were tightened to each implant analogue with a torque of 32 N·cm. The abutment-implant complexes were divided into two groups based on the presence or absence of attached mechanical retentive devices on zirconia frameworks (n=44 and 22, respectively).

These complexes were scanned using a laboratory scanner (D2000, 3Shape, Copenhagen, Denmark), and the frameworks were designed with 0.5 mm thickness using software (3Shape Dental Designer, 3Shape). Based on the designed standard triangulated language (STL) data, the frameworks were machine-milled from a pre-sintered zirconia disk (Katana Zirconia HT, Kuraray Noritake Dental, Tokyo, Japan) using a milling device (DWX-4, Roland, Shizuoka, Japan) and subsequently sintered in a furnace at 1,375°C for 90 min.

Protocol for attaching mechanical retentive devices

The surface of the zirconia frameworks was airborne-particle abraded with 50 μm Al_2O_3 particles (Hi-Alumina, Shofu, Kyoto, Japan) at a pressure of 0.2 MPa for 10 s, with 10 mm distance between the nozzle and framework surface (Fig. 1A). The mechanical retentive devices (FUJI Zircon beads FZB-100, Fuji Manufacturing, Tokyo, Japan) were adjusted to a particle size of 160-180 μm using a sieve (Test sieves JIS Z 8801, Tokyo Screen, Tokyo, Japan). The protocol for attaching different materials of mechanical retentive devices was divided into two groups. The glaze material (Cerabien ZR E glaze, Kuraray Noritake Dental) or the opaque porcelain material (Cerabien ZR SBA2, Kuraray Noritake Dental) was thinly applied onto the surface of the zirconia framework, referred to as the GL group and the OP group, respectively (Fig. 1B). The mechanical retentive devices were then sprinkled onto the glaze material or the opaque porcelain material from above on each axial surface of the zirconia framework while it was rotating (Fig. 1C). Then, the excess mechanical retentive devices were removed by gentle vibration with an equipment (Ceracon II, Shofu) (Fig. 1D). The sprinkled mechanical retentive devices were flattened using a fine brush to achieve a thickness of approximately one layer on the surface of the framework (Fig. 1D). The frameworks were fired according to the firing schedule outlined in Table 2 (Fig. 1E). The group with no attached mechanical retentive devices (ND group) underwent only airborne-particle abrasion (Fig. 1A). The fabricated frameworks are shown in Fig. 2.

Layering protocol

Feldspathic porcelain (Cerabien ZR, Kuraray Noritake Dental) and indirect composite resin (Estenia C&B, Kuraray Noritake Dental) were employed as layering materials (Table 1). The feldspathic porcelain was manually layered onto the frameworks and subsequently fired using a SingleMat porcelain furnace (Shofu) following the instructions provided by the manufacturer (FP veneer) (Fig. 1F). For the IC veneer, the frameworks were layered with Estenia C&B, cured using a photopolymerizer (α-light II, J. Morita, Suita, Japan), and heat-activated polymerized in an oven (KL-310, J. Morita) (Fig. 1G). Restorations were fabricated to achieve a standardized configuration with a width of 10.5 mm and a height of 8 mm using a standardized silicone index (Fig. 3).

Bonding protocol

The internal surfaces of the zirconia crowns and the surfaces of the implant abutments were airborne-particle abraded at a pressure of 0.2 Mpa and 0.5 Mpa, respectively. After the airborne-particle abrasion, both surfaces were primed (Clearfil Ceramic Primer Plus, Kuraray Noritake Dental). The crowns were then adhesively placed to the implant abutments using a dual-polymerized resin luting material (Panavia V5, Kuraray Noritake Dental). All specimens were restored in distilled water at 37°C for 24 h before undergoing fracture resistance testing.

Fracture resistance testing

A piece of tin foil was inserted between a stainless-steel ball (diameter, 6.0 mm) and the occlusal surface of the specimens. To determine fracture load, all specimens were subjected to perpendicularly loading using a mechanical testing machine (Type 5567, Instron, Canton, MA, USA) at a cross-head speed of 0.5 mm/min until fracture occurred. The break detector threshold was established at a 10% decrease of maximum force[25)].

Statistical analysis

The distribution and equality of variances were analyzed with the Shapiro-Wilk and Levene tests, using IBM SPSS Statistics (version 27.0, IBM, Armonk, NY, USA). The Shapiro-Wilk test indicated a normal distribution of the data ($p>0.05$), and the Levene test showed the homogeneity of variances ($p>0.05$). To compare the fracture load, Tukey's honestly significant difference test was employed within the same layering material group. A significance level of 0.05 was chosen for all data analyses.

Fracture pattern assessment

To examine the failure pattern, the fractured surfaces were observed under a stereomicroscope (Stemi DV4, Carl Zeiss, Jena, Germany). There were three types of fracture patterns, namely, veneer fracture, interface fracture, and framework fracture. Furthermore, the fractured surfaces were coated with a thin layer of gold using a sputter coater (Quick Coater Type SC-701, Sanyu Electron, Tokyo, Japan) for 30 s. The coated cross-sectional fractured surfaces and fractured surfaces were then examined using a scanning electron microscope (SEM) (ERA-8800FE, Elionix, Tokyo, Japan) at an operating voltage of 10 kV.

Results

The results of the descriptive statistical analysis for fracture load values and fracture patterns are summarized in Table 3. In the FP veneer, the GL group recorded the highest mean fracture load values of 3.00±0.28 kN. The mean fracture load values of the ND group (2.48±0.41 kN) were significantly higher than those of the OP group (1.91±0.48 kN). In the IC veneer, Tukey's honestly significant difference test revealed that the GL (2.62±0.22 kN) and OP (2.88±0.36 kN) groups had significantly higher mean fracture loads than the ND (2.19±0.34 kN) group.

The assessment of the failure pattern of the tested specimens indicated that the framework fracture was frequently observed in the GL and ND groups, irrespective of the veneer used (Table 3), as shown in Figs. 4a, 4c, 4d, and 4f. For the OP groups, a similar occurrence of interface fractures and framework fractures was observed for FP and IC veneers. Figures 4b and 4e show the interface fracture pattern of the OP group for the FP and IC veneers, respectively.

Representative stereomicroscopic images of the fracture surfaces are presented in Fig. 5. For the FP veneer-GL group, the cracked surface of the mechanical retentive devices surrounded by glaze material can be seen (Fig. 5a). The fracture surface of the FP veneer-OP group exhibited the mechanical retentive devices debonded from the opaque porcelain material (Fig. 5b). In Fig. 5c, which represents the FP veneer-ND group, mixed cohesive fractures of the frameworks and veneers are presented. Similar fracture surface images to those in the FP groups were observed in the IC groups (Figs. 5d-5f).

Representative SEM images of cross-sectional fractured surfaces in each group are shown in Fig.6. In the FP veneer-GL group, SEM images showed that the materials penetrated the undercut of the mechanical retentive devices at the interface between the zirconia framework and the layering material, as shown in Fig. 6a. Conversely, the SEM image of the FP veneer-OP group indicated the absence opaque porcelain material around the mechanical retentive devices (Fig. 6b). The SEM images of the FP veneer-ND group exhibited a directly contacting interface between the zirconia framework and the feldspathic porcelain (Fig. 6c).

For the IC veneers, the IC veneer-GL and OP groups showed that the mechanical retentive devices were embedded in the glaze and opaque porcelain materials, respectively (Figs. 6d and 6e). Figure 6f presents an image of the continuous interface between the zirconia framework and the indirect composite resin.

Figure 7 shows representative SEM images of fractured framework surfaces for the GL and OP groups. The FP veneer-GL group showed the fractured surface of the mechanical retentive devices and the mechanical retentive devices in the glaze porcelain material (Fig. 7a). In contrast, the FP veneer-OP group exhibited the interface fracture between the opaque porcelain materials and the zircon beads (Fig. 7b). The IC veneer-GL and OP groups indicated fracture within the glaze and opaque porcelain materials (Figs. 7c and 7d, respectively).

Discussion

The current study investigated the influence of attaching mechanical retentive devices onto frameworks on the fracture resistance of IZCs. The results of the study indicated that the fracture load of the GL group was significantly higher than that of the OP and ND groups for the FP veneer. In the IC veneer, the GL and OP groups showed significantly higher fracture load values than the ND group. Therefore, the null hypothesis that attaching mechanical retentive devices onto zirconia frameworks would not affect the fracture load of IZCs was rejected.

The FP veneer-GL group exhibited significantly higher fracture load values than the

FP veneer-OP and -ND groups. These findings suggest that the fracture resistance of IZCs can be enhanced by applying a glaze material before attaching mechanical retentive devices for porcelain layering onto the zirconia frameworks. Yamamoto *et al*.[26)] reported that the glaze application to zirconia frameworks before layering porcelain significantly enhanced the shear bond strength between zirconia and layering porcelain. The application of glaze material can improve the interaction with zirconia and increase its wettability to receive the layering porcelain. On the other hand, several studies have evaluated the influence of opaque application to zirconia frameworks on the bond strength to layering porcelain and indicated that such application negatively affected the bond strength[27,28)]. Additionally, a previous study revealed instances of complete delamination and microspaces at the interface between zirconia frameworks and porcelain[28)]. Hence, the glaze material would play a positive role in improving the bond between the zirconia framework and the layering porcelain[26,29)], leading to increased overall fracture load of the IZCs. The glaze material applied to the zirconia surface provides a surface property similar to that of glass ceramics[29)]. This characteristic likely contributed to a stronger bond with the layering porcelain, leading to enhanced integration between the frameworks and veneers, which resulted in higher fracture load. The findings are supported by the observation in Fig. 5a, where the framework and layering material exhibit a strong bond, causing the zircon beads to fracture. Additionally, Figs. 6a and 7a indicates that the glaze material may have penetrated the undercut of the zircon beads, providing mechanical interlocking. These observations suggest that the GL group possesses enhanced fracture load compared to the OP and ND groups.

The mean fracture load values of the FP veneer-OP group were significantly lower than those of the FP veneer-ND group. Figure 5b shows that the entire zircon beads are detached from the fracture surface in the FP veneer-OP group. Additionally, Fig. 6b reveals the absence of layering material around the zircon beads and the presence of gaps at the interface. In addition, the interface fracture between the opaque porcelain materials and the zircon beads was observed in Fig.7b. These findings suggest that the fracture may have originated from the weak interface surrounding the mechanical retentive devices. One possible explanation for this finding is the difference in thermal expansion coefficients between the zircon beads (4.9×10^{-6}/°C) and the layering porcelain (8.9-9.1×10^{-6}/°C), which can be caused by repeated thermal cycling during the porcelain firing process[24,30,31].

For the IC veneer, the GL and OP groups exhibited significantly higher fracture load values than the ND group. Moreover, Figs. 6d and 6e displayed the infiltration of the layering materials into the undercut of mechanical retentive devices. SEM examination of fractured frameworks further revealed the fracture within the glaze and opaque porcelain materials (Figs. 7c and 7d). These results indicate that the mechanical retentive devices effectively enhanced mechanical interlocking between the zirconia frameworks and indirect composite materials in the GL and OP groups for the IC veneer. This is supported by the findings of previous studies, which demonstrated that the shear bond load between zirconia frameworks attached mechanical retentive devices and indirect composite resin was higher than that of the bond without the mechanical retentive devices[23,24]. There was no significant difference in fracture load between the GL and OP groups for the IC veneer. This could be because there was no thermal treatment after applying the mechanical retentive devices to the zirconia frameworks, resulting in the absence of variation in the porcelain material used to provide mechanical retentive devices between the two groups. The difference between the results of the FP and IC veneers may be attributed to the presence or absence of thermal stress that occurs during the layering procedures.

The mean fracture load values of the IZCs evaluated in the current study exceeded 1.91 kN, which is higher than the physiological average occlusal force of 0.45-0.57 kN in adults[32]. This demonstrates the potential for the clinical application of IZCs with mechanical retentive devices employed in the current study.

There are no studies available to verify the bond strength between zircon and glaze or opaque materials. The zircon beads used in this study contained 30% SiO_2, as indicated in Table 1. A method of coating zirconia beads with feldspathic porcelain and using them as mechanical retentive devices for zirconia frameworks has been introduced[33)]. Although the bond strength between zircon beads and glaze or opaque material has not been determined, it is hypothesized that the SiO_2 contained in the zircon beads may be effective in forming a strong interface between the zirconia and the layering material. In addition, a previous study has reported that a particle size of 180 µm was effective for a mechanical retentive device in terms of bond strength to metal frameworks[34)]. Thus, zircon beads with a particle size of 160-180 µm were used in this study. Within the limitations of the current *in vitro* study, it can be concluded that the fracture resistance of IZCs can be enhanced with mechanical retentive devices for porcelain or indirect composite resin layering onto the zirconia frameworks. Although the results of this *in vitro* study of IZCs attaching mechanical retentive devices to zirconia frameworks are promising, further *in vitro* investigations that incorporate artificial aging processes, such as thermal and fatigue cycling stress, need to be performed before the clinical application of such prostheses can be considered.

Conclusions

1. The fracture resistance of the IZCs can be improved by applying glaze material before attaching mechanical retentive devices for porcelain layering.
2. For the IC veneer, the GL and OP groups showed significantly higher fracture load values than the ND group.
3. The mechanical interlocking between the zirconia frameworks and the layering materials tested was achieved with the use of mechanical retentive devices.

4. All types of the IZCs tested in this study have the potential to withstand clinical occlusal forces in posterior applications.

References

1) Pjetursson BE, Sailer I, Latyshev A, Rabel K, Kohal RJ, Karasan D. A systematic review and meta-analysis evaluating the survival, the failure, and the complication rates of veneered and monolithic all-ceramic implant-supported single crowns. Clin Oral Implants Res 2021; 32: 254-288.

2) Pjetursson BE, Valente NA, Strasding M, Zwahlen M, Liu S, Sailer I. A systematic review of the survival and complication rates of zirconia-ceramic and metal-ceramic single crowns. Clin Oral Implants Res 2018; 29: 199-214.

3) Beuer F, Schweiger J, Eichberger M, Kappert HF, Gernet W, Edelhoff D. High-strength CAD/CAM-fabricated veneering material sintered to zirconia copings - a new fabrication mode for all-ceramic restorations. Dent Mater 2009; 25: 121-128.

4) Taguchi K, Komine F, Fushiki R, Blatz MB, Kamio S, Matsumura H. Fracture resistance of single-tooth implant-supported zirconia-based indirect composite-layered molar restorations. Clin Oral Implants Res 2014; 25: 983-991.

5) Honda J, Komine F, Kusaba K, Kitani J, Matsushima K, Matsumura H. Fracture loads of screw-retained implant-supported zirconia prostheses after thermal and mechanical stress. J Prosthodont Res 2020; 64: 313-318.

6) Mühlemann S, Lakha T, Jung RE, Hämmerle CHF, Benic GI. Prosthetic outcomes and clinical performance of CAD-CAM monolithic zirconia versus porcelain-fused-to-metal implant crowns in the molar region: 1-year results of a RCT. Clin Oral Implants Res 2020; 31: 856-864.

7) Aboushelib MN, de Kler M, van der Zel JM, Feilzer AJ. Effect of veneering method on

the fracture and bond strength of bilayered zirconia restorations. Int J Prosthodont 2008; 21: 237-240.

8) Lundberg K, Wu L, Papia E. The effect of grinding and/or airborne-particle abrasion on the bond strength between zirconia and veneering porcelain: a systematic review. Acta Odontol Scand 2017; 3: 8-20.

9) Saied MA, Lloyd IK, Haller WK, Lawn BR. Joining dental ceramic layers with glass. Dent Mater 2011; 27: 1011-1016.

10) Komine F, Strub JR, Matsumura H. Bonding between layering materials and zirconia frameworks. Jpn Dent Sci Rev 2012; 48: 153-161.

11) Fushiki R, Komine F, Blatz MB, Koizuka M, Taguchi K, Matsumura H. Shear bond strength between an indirect composite layering material and feldspathic porcelain-coated zirconia ceramics. Clin Oral Investig 2012; 16: 1401-1411.

12) Fushiki R, Komine F, Honda J, Kamio S, Blatz MB, Matsumura H. Long-term bond strength between layering indirect composite material and zirconia coated with silicabased ceramics. J Adhes Dent 2015; 17: 273-281.

13) Abdullah AO, Hui Y, Sun X, Pollington S, Muhammed FK, Liu Y. Effects of different surface treatments on the shear bond strength of veneering ceramic materials to zirconia. J Adv Prosthodont 2019; 11: 65-74.

14) Abdullah AO, Yu H, Pollington S, Muhammed FK, Xudong S, Liu Y. Effect of repeated laser surface treatments on shear bond strength between zirconia and veneering ceramic. J Prosthet Dent 2020; 123: 338.e1-338.e6.

15) Henriques B, Fabris D, Souza JCM, Silva FS, Carvalho Ó, Fredel MC, *et al*. Bond strength enhancement of zirconia-porcelain interfaces via Nd:YAG laser surface structuring. J Mech Behav Biomed Mater 2018; 81: 161-167.

16) Kirmali O, Akin H, Ozdemir AK. Shear bond strength of veneering ceramic to zirconia

core after different surface treatments. Photomed Laser Surg 2013; 31: 261-268.

17) Kirmali O, Kapdan A, Kustarci A, Er K. Veneer ceramic to Y-TZP bonding: comparison of different surface treatments. J Prosthodont 2016; 25: 324-329.

18) Conserva E, Menini M, Tealdo T, Bevilacqua M, Ravera G, Pera F, *et al*. The use of a masticatory robot to analyze the shock absorption capacity of different restorative materials for prosthetic implants: a preliminary report. Int J Prosthodont 2009; 22: 53-55.

19) Demarco FF, Corrêa MB, Cenci MS, Moraes RR, Opdam NJ. Longevity of posterior composite restorations: not only a matter of materials. Dent Mater 2012; 28: 87-101.

20) Zenthöfer A, Rammelsberg P, Schmitt C, Ohlmann B. Wear of metal-free resin composite crowns after three years in service. Dent Mater J 2013; 32: 787-792.

21) Shue SL, Nicholls JI, Townsend JD. The effect of metal retentive designs on resin veneer retention. J Prosthet Dent 1987; 58: 297-305.

22) Muratomi R, Kamada K, Taira Y, Higuchi S, Watanabe I, Sawase T. Comparative study between laser sintering and casting for retention of resin composite veneers to cobalt-chromium alloy. Dent Mater J 2013; 32: 939-945.

23) Matsushima K, Kubochi K, Komine F, Kimura F, Kobayashi T, Matsumura H. Bond strength between a veneering composite resin and zirconia frameworks with attached mechanical retentive devices. Dent Mater J 2022; 41: 117-125.

24) Ohira C, Taira Y, Takenaka H, Fukui J, Kamada K, Sawase T. Effects of ceramic microbeads on bonding between a zirconia framework and layered resin composite. Dent Mater J 2023; 42: 516-522.

25) Behr M, Rosentritt M, Latzel D, Kreisler T. Comparison of three types of fiber-reinforced composite molar crowns on their fracture resistance and marginal adaptation. J Dent 2001; 29: 187-196.

26) Yamamoto LT, Rodrigues VA, Dornelles LS, Bottino MA, Valandro LF, Melo RM. Low-fusing porcelain glaze application on 3Y-TZP surfaces can enhance zirconia-porcelain adhesion. Braz Dent J 2016; 27: 543-547.

27) Ishibe M, Raigrodski AJ, Flinn BD, Chung KH, Spiekerman C, Winter RR. Shear bond strengths of pressed and layered veneering ceramics to high-noble alloy and zirconia cores. J Prosthet Dent 2011; 106: 29-37.

28) Kim HJ, Lim HP, Park YJ, Vang MS. Effect of zirconia surface treatments on the shear bond strength of veneering ceramic. J Prosthet Dent 2011; 105: 315-322.

29) Valentino TA, Borges GA, Borges LH, Platt JA, Correr-Sobrinho L. Influence of glazed zirconia on dual-cure luting agent bond strength. Oper Dent 2012; 37: 181-187.

30) Anusavice KJ, DeHoff PH, Hojjatie B, Gray A. Influence of tempering and contraction mismatch on crack development in ceramic surfaces. J Dent Res 1989; 68: 1182-1187.

31) Swain MV. Unstable cracking (chipping) of veneering porcelain on all-ceramic dental crowns and fixed partial dentures. Acta Biomater 2009; 5: 1668-1677.

32) Nimura K, Shiga H, Yokoyama M. Relationships of physical constitution with occlusal force and masticatory performance in adults with natural dentition. Odontology 2023; 111: 1018-1024.

33) Taira Y, Fukui J, Sawase T. Silica-fused zirconia micro beads for retention between veneering resin composite and zirconia. J Dent Oral Biol 2017; 2: 1099.

34) Tanaka T, Atsuta M, Uchiyama Y, Nakabayashi N, Masuhara E. Spherical powder for retaining thermosetting acrylic resin veneers. J Prosthet Dent 1978; 39: 295-303.

Tables and Figures

Table 1 Materials used in the current study

Material (Trade name)	Lot no.	Components	Manufacturer
Implant Implant replica Brånemark System WP	401165	Stainless steel	Nobel Biocare, Goteborg, Sweden
Abutment Snappy abutment 5.5 Brånemark System WP	13132474	Ti-6Al-4V	Nobel Biocare
Abutment screw Abutment screw 5.5 Brånemark System WP	13132474	Ti-6Al-4V	Nobel Biocare
Zirconia ceramic material Katana Zirconia HT	EENBK	ZrO_2 94.4%, Y_2O_3 5.4%, others	Kuraray Noritake Dental, Tokyo, Japan
Mechanical retentive devices FUJI Zircon beads FZB-100		ZrO_2 65%, SiO_2 30%, Al_2O_3 <10%	Fuji Manufacturing, Tokyo, Japan
Feldspathic porcelain Cerabien ZR (SBA2, A2B, E2, E glaze)	DTRZL, EFNPM, EATUK, EEVQZ	SiO_2, Al_2O_3, K_2O, Na_2O, others	Kuraray Noritake Dental
Indirect composite resin Estenia C&B (OA2, DA2, E2)	330025 970031 320046	UTMA, Bis-GMA, methacrylate, photoinitiator, pigment, filler	Kuraray Noritake Dental
Priming agent Clearfil Ceramic Primer Plus	790066	3-TMSPMA, MDP, ethanol	Kuraray Noritake Dental
Luting agent Panavia V5	AJ0176	PasteA: Bis-GMA, TEGDMA, hydrophobic aromatic dimethacrylate, hydrophilic aliphatic dimethacrylate, initiators, accelerators, silanized fluoroaluminosilicate glass filler, colloidal silica Paste B: Bis-GMA, hydrophobic aromatic dimethacrylate, hydrophilic aliphatic dimethacrylate, initiators, accelerators, silanized fluoroaluminosilicate glass filler, silanized aluminum oxide filler, accelerators, CQ, pigments	Kuraray Noritake Dental

UTMA, urethane tetramethacrylate; Bis-GMA, bisphenol A-diglycidyl methacrylate; TMSPMA, 3-trimethoxysilylpropyl methacrylate; MDP, 10-methacryloyloxydecyl dihydrogen phosphate; TEGDMA, triethyleneglycol dimethacrylate; CQ, *dl*-camphorquinone.

Table 2 The firing schedule

	Pre-drying					
	Temperature (°C)	Time (min)	Heating rate (°C/min)	Firing temperature	Holding time (min)	Cooling time (min)
Glaze material	600	5	65	850	1	4
Opaque porcelain material	600	5	45	930	1	4

Table 3 Fracture load values (kN) and fracture patterns for the tested specimens

Veneer	Group	Mean±SD*	Category**	Fracture pattern, no. of specimens		
				V	I	F
FP	GL	3.00±0.28	A	0	4	7
	OP	1.91±0.48	C	0	6	5
	ND	2.48±0.41	B	0	3	8
IC	GL	2.62±0.22	a	0	4	7
	OP	2.88±0.36	a	0	6	5
	ND	2.19±0.34	b	0	4	7

FP, feldspathic porcelain; IC, indirect composite resin; GL, attaching mechanical retentive devices using glaze material; OP, attaching mechanical retentive devices using opaque porcelain material; ND, no attaching mechanical retentive devices; V, veneer fracture; I, interface fracture; F, framework fracture.
*Standard deviation.
**Different uppercase letters indicate a statistically significant difference in the FP veneer; different lowercase letters indicate a statistically significant difference in the IC veneer (Tukey's HSD test, $p<0.05$).

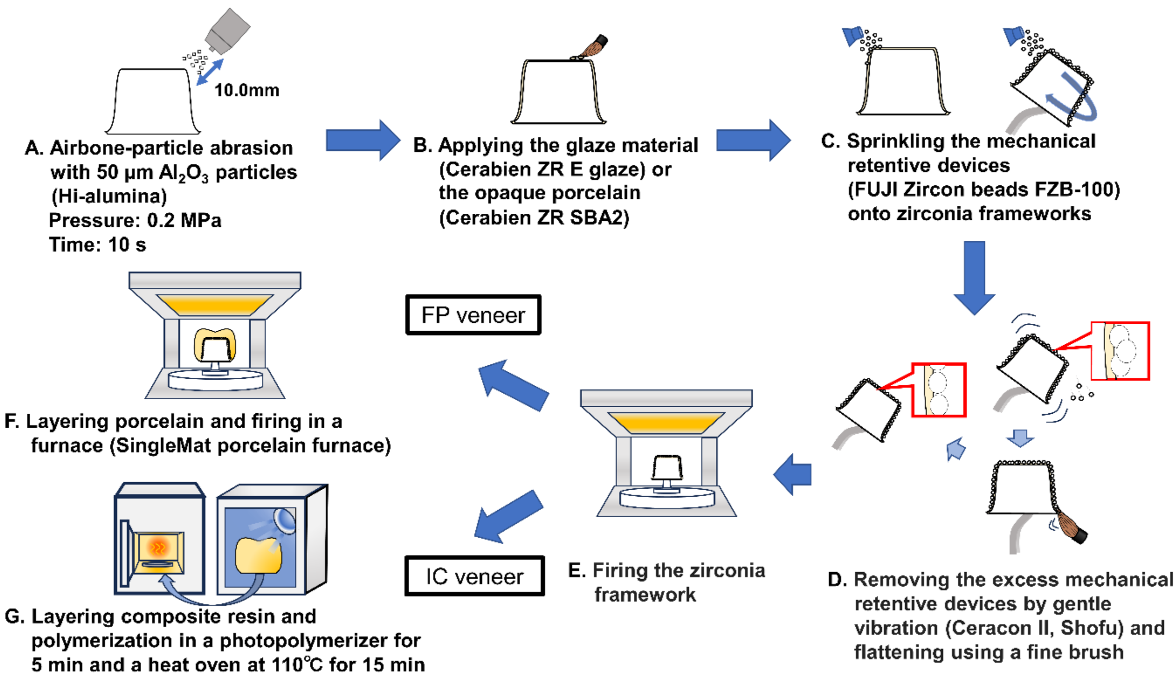

Fig. 1 Flowchart of mechanical retentive devices attachment

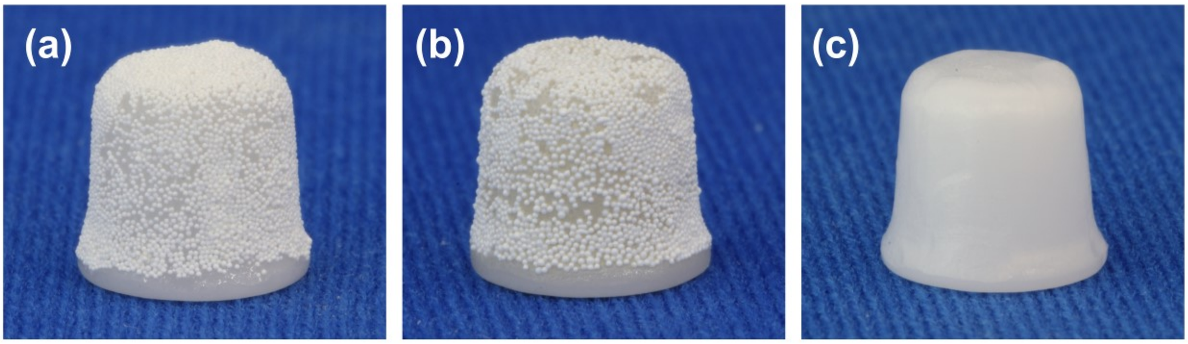

Fig. 2 Representative frameworks: (a) GL, (b) OP, and (c) ND groups

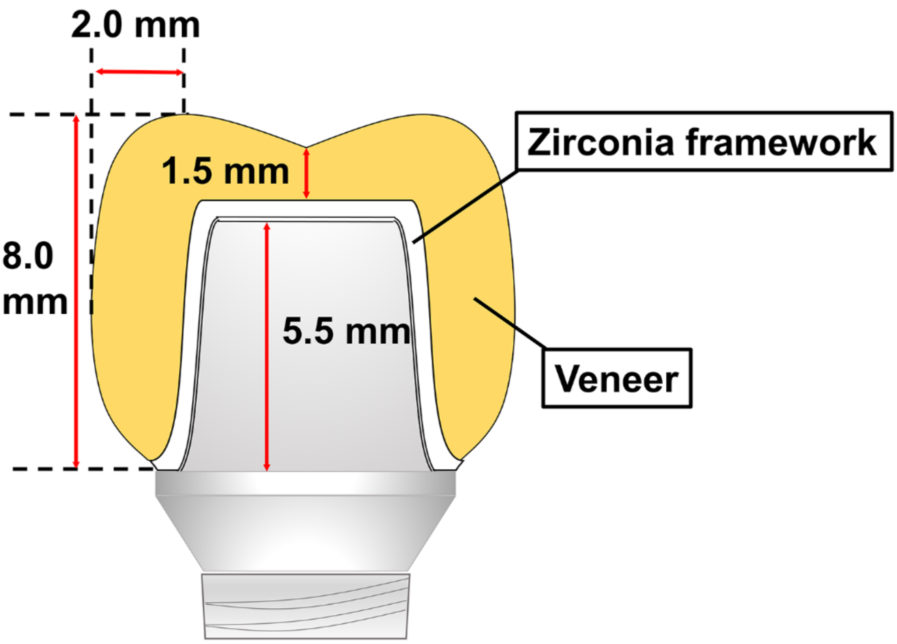

Fig. 3 Schematic representations of the specimens

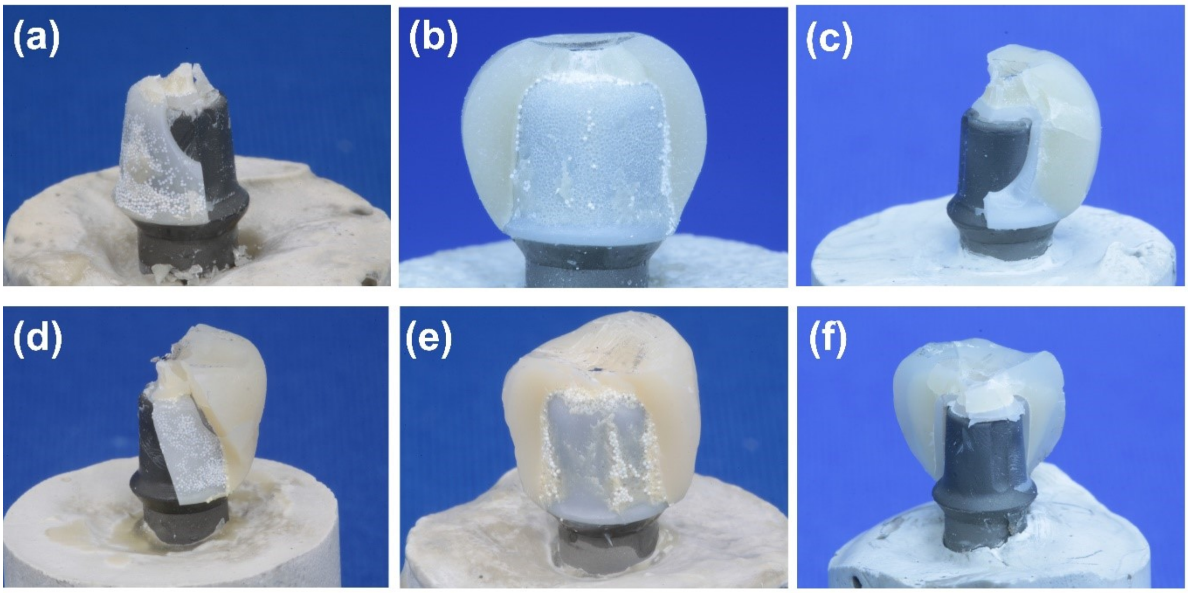

Fig. 4 Representative specimens in each group after fracture resistance testing: (a) the FP veneer-GL group, (b) the FP veneer-OP group, (c) the FP veneer-ND group, (d) the IC veneer-GL group, (e) the IC veneer-OP group, and (f) the IC veneer-ND group.

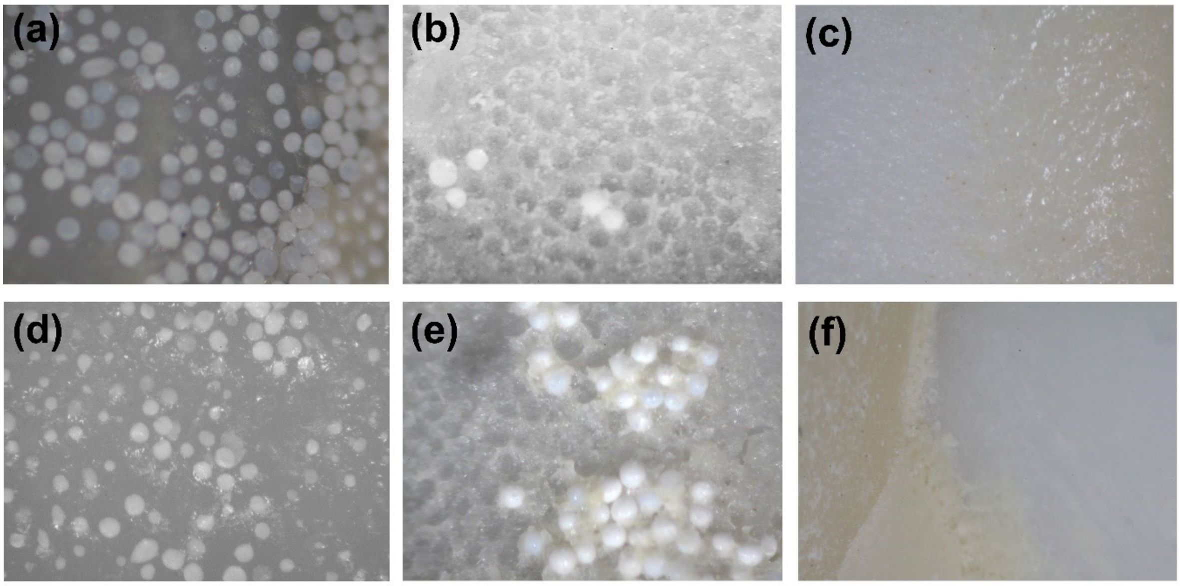

Fig. 5 Representative stereomicroscopic images of fractured surfaces in each group (original magnification ×32): (a) the FP veneer-GL group, (b) the FP veneer-OP group, (c) the FP veneer-ND group, (d) the IC veneer-GL group, (e) the IC veneer-OP group, and (f) the IC veneer-ND group.

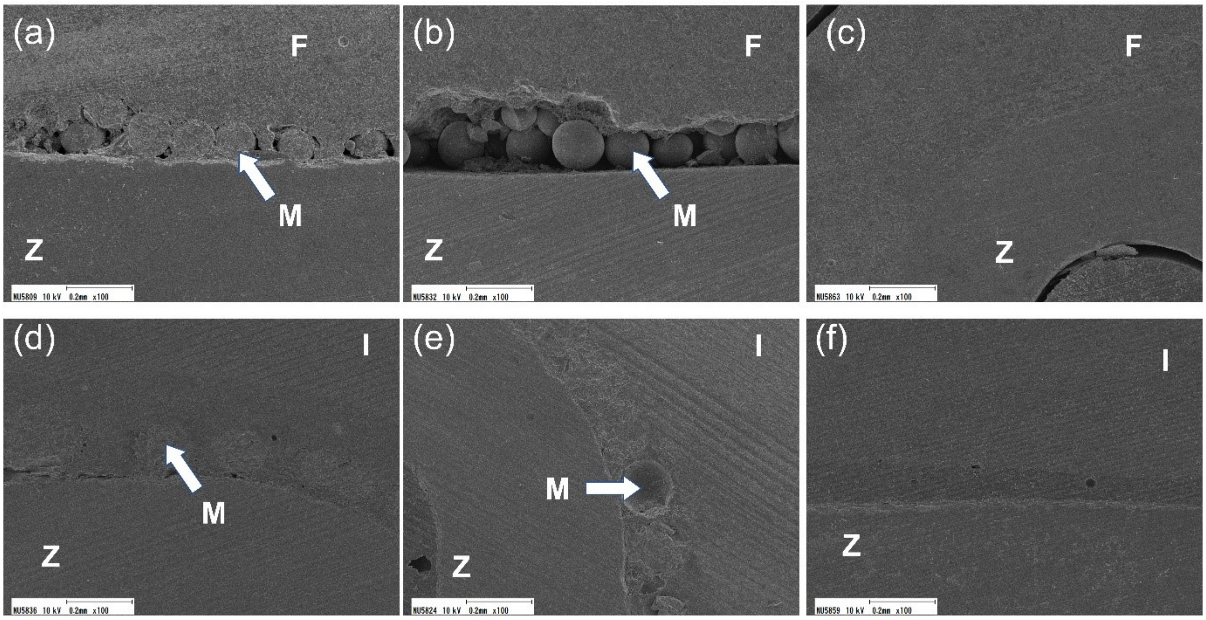

Fig. 6 Representative SEM images of cross-sectional fractured surfaces in each group (original magnification ×100): (a) the FP veneer-GL group, (b) the FP veneer-OP group, (c) the FP veneer-ND group, (d) the IC veneer-GL group, (e) the IC veneer-OP group, and (f) the IC veneer-ND group. F, feldspathic porcelain; I, indirect composite resin; M, mechanical retentive device; Z, zirconia.

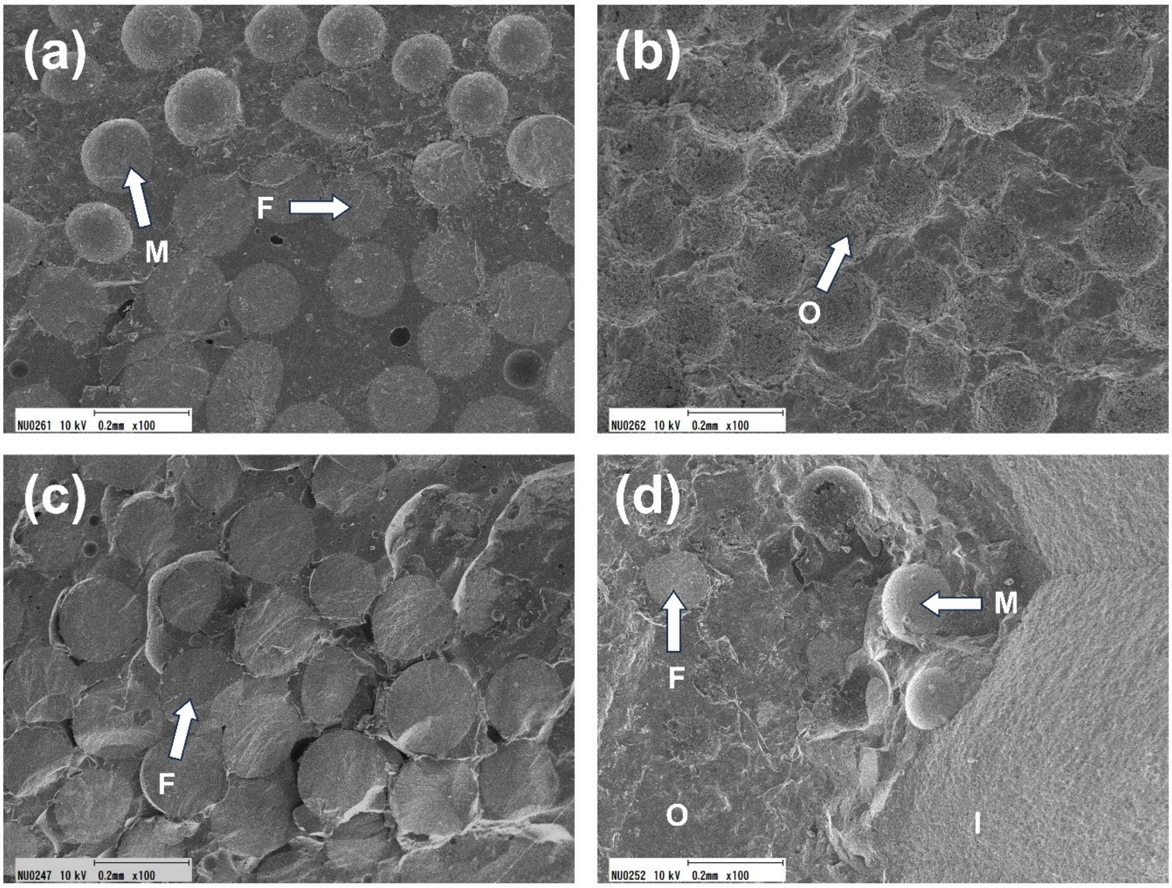

Fig. 7 Representative SEM images of fractured framework surfaces for the GL and OP groups. (original magnification ×100): (a) the FP veneer-GL group, (b) the FP veneer-OP group, (c) the IC veneer-GL group, and (d) the IC veneer-OP group. F, fractured surface of mechanical retentive device; I, indirect composite resin; M, mechanical retentive device; O, opaque porcelain material.